

07,11,14

## Estimating the Dimensions of Nanocrystalline Elements of the Polyethylene Structure by Differential Scanning Calorimetry

© V.M. Egorov<sup>1</sup>, A.K. Borisov<sup>1</sup>, V.A. Marikhin<sup>1</sup>, L.P. Myasnikova<sup>1</sup>, S.A. Gurieva<sup>1</sup>, E.M. Ivankova<sup>2</sup>

<sup>1</sup> Ioffe Institute,  
St. Petersburg, Russia

<sup>2</sup> Institute of Macromolecular Compounds, Russian Academy of Sciences,  
St. Petersburg, Russia

E-mail: victor\_egorov1@inbox.ru

Received April 28, 2022

Revised April 28, 2022

Accepted May 2, 2022

A method is proposed for calculating the dimension distribution of nanocrystalline elements of the lamellar and fibrillar morphologies of a polymer. Calorimetric data were used to calculate the distribution of the longitudinal size of these elements in lamellae and microfibrils of ultrahigh molecular weight polyethylene. The calculation results are consistent with the data obtained by the X-ray method.

**Keywords:** heat capacity, dimension effect, lamella, microfibril, polyethylene.

DOI: 10.21883/PSS.2022.08.54623.369

### 1. Introduction

Over the last decade, significant advances have been made in the development of structural materials for applications requiring increased mechanical properties and high levels of operational reliability for products made from these materials. Such materials include highly oriented ultrahigh molecular weight polyethylene (HMWPE) fibers and filaments produced using gel technology. These materials exhibit very high strength and elastic modulus values [1,2], while retaining significant growth potential, as the values achieved are well below theoretical estimates [3]. It is important to note that UHMWPE gel fibers hold the record for specific performance (per unit mass of material) among all types of modern ultra high-strength structural materials.

In order to practically harness the „growth potential“, it is necessary to find out the physical reasons that inhibit this growth. Since there is a correlation between the mechanical properties of polymeric materials and the per molecular structure (PMC), it is necessary to elucidate the patterns of PMC formation at each stage of fiber production. In the present work, a method based on differential scanning calorimetry (DSC) melting curve shape analysis is proposed to obtain data on the size distribution of nanocrystalline formations in a polymer with different PMC, including lamellar and fibrillar structures.

### 2. Materials and experimental techniques

In the work, thermal physical characteristics of different samples were investigated: an initial xerogel film obtained from a 1% solution in mineral oil of a centrifugal HMWPE powder with an average viscosity molecular mass  $Mw = 3 \cdot 10^6$ , and filaments with different degrees

of stretching obtained by a multi-step zone orientation hardening of the initial film on local heaters [4]. The samples listed above were examined with a Zeiss SUPRA 55 VP electron microscope and a DSC PerkinElmer calorimeter.

### 3. Discussion

Fig. 1 shows electron microscopic images of the original xerogel and oriented films showing the evolution of the PMC polymer during orientation. Thus, an image of the original xerogel (Fig. 1, *a*) shows typical lamellar formations, which are multi-layered stacks of nanometre-thick lamellae of folded macromolecules. During orientation stretching, a radical rearrangement of the original lamellar structure into a new macro- and microfibrillar organization occurs as a result of recrystallisation with the unfolding of the folded structure and the formation of a new one from the straightened molecules. Fibrils occur during the initial stages of drawing in the „neck“ area (degree of elongation  $\lambda = 10-15$ , where  $\lambda = x/x_0$ ,  $x_0$  — original sample size,  $x$  — sample size after drawing), that is, an abrupt local contraction of the sample. This still leaves islets with an undirected lamellar morphology (Fig. 1, *b*), which will be converted to microfibrils during the subsequent drawing stages. The transverse dimensions of the microfibrils are 30–0 nm and the lengths of the microfibrils can reach several micrometers. Microfibrils are heterogeneous in length: there is a periodic alternation of ordered three-dimensional crystal areas of nanometer size and defective areas (otherwise known as disordered), consisting of so-called „tie“ molecules that connect the crystal areas. The tie molecules contain a large number of conformational defects of various types, which determine the degree of their curvature.

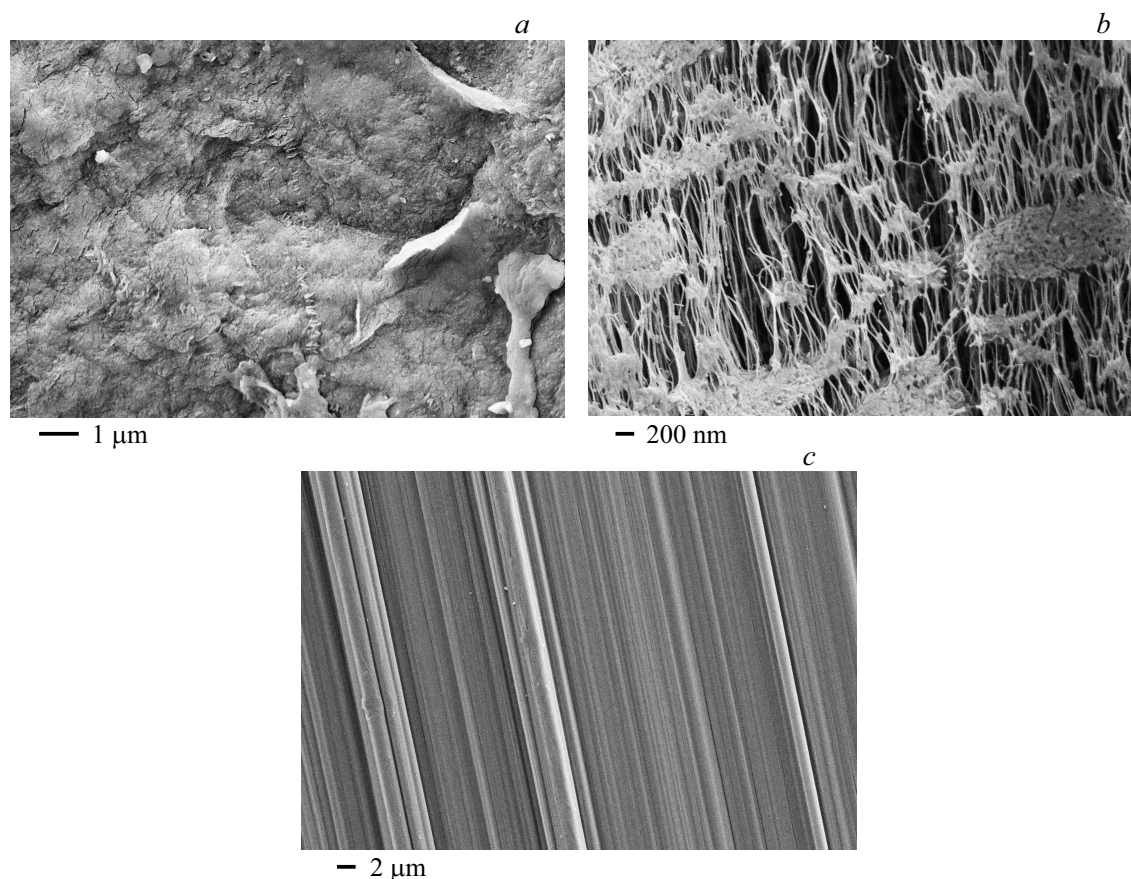


**Figure 1.** Microphotographs of xerogel obtained from a 1.5% solution in Vaseline oil (*a*), oriented film in the neck area ( $\lambda = 15$ ) (*b*), oriented film ( $\lambda = 77$ ) (*c*).

The samples are further stretched by plastic deformation (sliding) of the formed microfibrils against each other. The structure of the disordered intra-fibrillar areas is changed by the shear forces that develop during the sliding of the fibrils. The elongation limits can reach very high values, up to several hundred  $\lambda$ . The image (Fig. 1, *c*) shows a microphotograph of an oriented HMWPE film with elongation degree  $\lambda = 77$ . Macrofibrils — bundles of microfibrils oriented along the orientation axis of the film can be seen. Their cross-sectional size is larger than the diameter of the microfibrils observed in the „neck“ microphotograph.

Fig. 2 shows the DSC curves of the studied objects, which demonstrate the character of the melting peak parameters change with orientation. It can be seen that the temperature of the maximum endothermic melting peak  $T_{\max}$  increases with increasing  $\lambda$ . The shape of the peak also changes significantly: the amplitude increases, and in the first stage ( $\lambda < 50$ ) a low-temperature wing is observed. At higher degrees of orientation the wing disappears and the enthalpy of melting  $\Delta H$  and thus the degree of crystallinity increase at higher  $\lambda$  by 10–30%. It is clear that changes in the quantitative characteristics of the melting peak reflect the radical rearrangement of the PMC that occurs in the

polymer during orientation. First and foremost, this applies to crystalline formations whose melting point varies within a very wide melting temperature range. Apparently, these crystal formations differ in size, because in terms of internal structure they are identical, as they are formed by the same methylene groups  $-\text{CH}_2-$ . In this case, the temperature range and shape of the endothermic melting peak must be related to the size distribution of the crystal formations.

The method that we propose to derive the size distribution of crystalline formations in the polymer from the analysis of DSC curves is based on the fact that the heat flux on DSC melting curves is proportional to the mass fraction of crystallites melting as a function of size at a given temperature. In this case, the heat flux as a function of temperature is converted into a heat flux distribution as a function of the longitudinal size of the crystallite according to the following relation [5]:

$$dH/dl_1 = (dT/dl_1)(dH/dT), \quad (1)$$

where  $dH/dT$  — is the experimental dependence of heat capacity on temperature, determined from the DSC curve taking into account the temperature scan rate;  $l_1$  — the longitudinal size of the crystallite, equal to  $l_1 = h \times n$ , where  $n$  — the number of C–C bonds of the main chain,

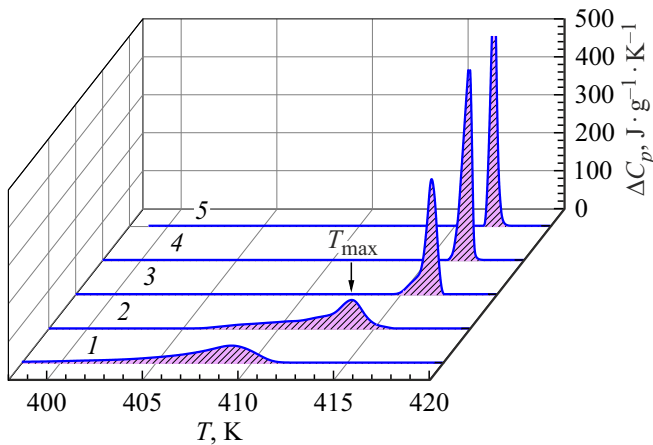


**Figure 2.** DSC curves of HMWPE samples obtained by heating ( $V = 5 \text{ K/min}$ ): curve 1 — original film; oriented HMWPE with elongation degree  $\lambda = 9$  (curve 2),  $\lambda = 43$  (curve 3),  $\lambda = 95$  (curve 4),  $\lambda = 170$  (curve 5).

$h$  — the bond projection length on the macromolecule axis (for polyethylene  $h = 0.124 \text{ nm}$ ). The dependence  $dT/dl_1$  is determined by a generalized Gibbs-Thomson equation based on a balance of surface and bulk energies [6,7]:

$$T(l_1) = T_0 [1 - 2/\Delta H_0 (\sigma/l_2 + \sigma/l_3 + \sigma_e/l_1)], \quad (2)$$

where  $l_2$  and  $l_3$  — dimensions of the crystallite in the cross section plane perpendicular to the longitudinal axis coinciding with the direction of the macromolecule;  $\sigma$  — surface energy of the lateral surfaces of the crystallite;  $\sigma_e$  — the surface energy of the end surface;  $\Delta H_0 = 293 \text{ J/cm}^{-3}$  and  $T_0 = 415 \text{ K}$  — the heat and melting point of an ideal polyethylene crystal [6].

Before using relations (1) and (2) to calculate the distribution from the experimental DSC curves shown in Fig. 2, the methodological error  $\Delta T$  in determining the current value  $T$  must be considered, since with a small difference  $T_0 - T$  the error in determining  $l_1$  may be significant. It is commonly known that method error of the DSC-method (offset of temperature peak by  $\Delta T$ ) arises due thermo-resistance  $R$  of the sample under test in a calorimetric cell. It turns out that the error magnitude can be determined as follows: since the value of  $\Delta T$  depends on the sample mass  $m$  and scanning speed  $V$  by the relation  $\Delta T = R(mV)^{1/2}$  [8], it is necessary to plot the dependence  $T_{\max} = f(V^{1/2})$  from experimental data obtained by varying the heating speed  $V$ , which should be linear in the absence of structural transformation in sample during temperature scanning. Then extrapolating the linear relation obtained in the experiment to  $V \rightarrow 0$  allows us to determine the methodological error  $\Delta T$ , which in our case is  $\Delta T = 1.6 \text{ K}$ .

The Thomson–Gibbs equation in simplified form is often used to determine the average thickness of lamellae for which parameters  $l_2$  and  $l_3 \gg l_1$ , so the terms  $\sigma/l_2$  and  $\sigma/l_3$  are neglected in expression (2). Since in the original

xerogel film the permolecular structure of HMWPE consists of stacks of lamellae, a simplified expression

$$T(l_1) = T_0 [1 - 2\sigma_e/\Delta H_0 l_1] \quad (3)$$

can be used to calculate the distribution  $dH/dl_1$  using relations (1) and (3). However, this distribution is not a distribution of the number of lamellas by thickness, as thicker lamellas absorb more heat. This distribution cannot be compared with the distribution obtained by other methods which fix the number of lamellae of a certain thickness. Therefore, to determine the number of lamellas of a certain thickness, it is necessary to normalize by  $l_1$ , i.e. calculate  $l_1^{-1} \cdot dH/dl_1$ . Figure 3 (curve 1) shows this calculation in percentage terms for the original undirected sample. In the calculation, the surface energy value  $\sigma_e = 9 \cdot 10^{-6} \text{ J/cm}^2$  [6] was used. The figure shows that the maximum number of lamellae is in the 6–8 nm range (18%). Note also that the bulk of the lamellas ( $\sim 80\%$ ) are in lamella thicknesses from 4 to 14 nm.

It was noted above that the permolecular lamellar structure of the original xerogel film undergoes a radical change during mechanical drawing: the lamellar structure is rearranged into a fibrillar [1] structure. As is known [3], the PMC of a fibril consists of a successive alternation of crystalline and disordered areas in which most of the macromolecules coming out of the previous crystallite enter the subsequent one. For fibrils, the parameters  $l_2$  and  $l_3$  of the crystal areas are comparable to  $l_1$ , so the generalized Gibbs-Thomson equation (2) must be used to determine the relations  $T(l_1)$  by first determining the surface energy values of the lateral and end faces, that is,  $\sigma$  and  $\sigma_e$ . It should be noted that in the case of an orthorhombic HMWPE lattice the lateral surface energy coincides completely only at the two opposite faces, differing slightly from the surface energy of the adjacent lateral surfaces. Therefore, it is possible

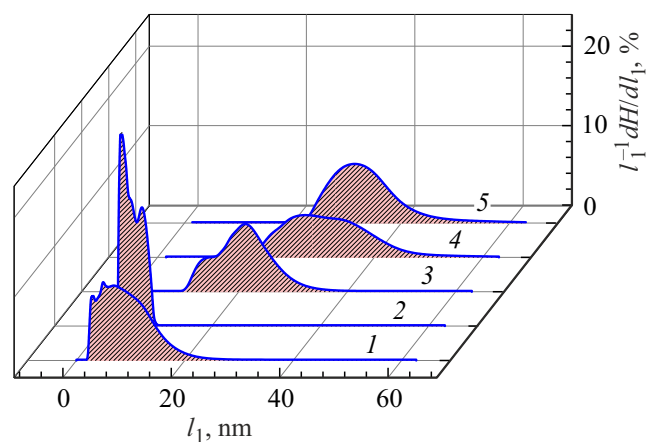


**Figure 3.** Dependences of the number of crystal formations on the longitudinal size of these formations, expressed as a percentage. Curve 1 — original film; oriented HMWPE with elongation degree  $\lambda = 9$  (curve 2),  $\lambda = 43$  (curve 3),  $\lambda = 95$  (curve 4),  $\lambda = 170$  (curve 5).

to assume in the first approximation the surface energy is the same at all lateral surfaces and then use only the end face  $\sigma_e$  and lateral  $\sigma$  surface energies. From now on, for simplicity, crystallites with cross-sectional dimensions of sides  $l_2 = l_3 = l$  and length  $l_1$  in the chain direction will be considered, so expression (2) takes the following form:

$$T(l_1) = T_0[1 - 2/\Delta H_0(2\sigma/l + \sigma_e/l_1)]. \quad (4)$$

The lateral surface energy  $\sigma$  in microfibrils is related to the interaction energy of the microfibrils with each other within the microfibril. Microfibrils interact with each other by weak cohesive forces of intermolecular interaction. This is confirmed by the effect that can be observed visually — when tensile stress is applied perpendicular to the axis of the microfibril, it splits very easily at the boundaries between the microfibrils.

To determine the surface energy  $\sigma$ , i.e. the intermolecular interaction energy per unit area  $\sim 0.2 \text{ nm}^2$  of the methylene group  $-\text{CH}_2-$  of the lateral surface of the chain, one must determine the fraction of the cohesion energy  $E_c = 3.6 \text{ kJ/mol}$  [9] that accounts for the van der Waals interaction in the disordered phase. It is known [9] that this proportion is  $(0.35 \pm 0.05)E_c$ . Estimating from the above parameters gives a lateral surface energy value equal to  $\sigma \approx 9 \text{ erg/cm}^2$ .

It is more difficult to correctly determine the value of the end-surface energy  $\sigma_e$ , which is formed in intergranular disordered areas. It should be noted that it is the structure of the intergranular disordered areas that control the mechanical strength of the oriented polymer. There are several models [10] that focus on the details of the structure of intergranular disordered areas. Fig. 4 schematically shows the most important of them, a detailed analysis of which is necessary to elucidate the picture of the formation of the end surface energy of crystallites.

Let us consider the occurrence of the elements shown in Figure 4:

1 — crystalline bridges or fully straightened molecules in trans-conformation between neighboring crystallites in the microfibril (Fig. 4, position 1). The presence of such crystalline bridges is confirmed by X-ray diffraction studies, which show that the effective average crystallite size exceeds the value of the large period, which can be explained by the considerable number of straightened molecules in disordered areas of the microfibrils [11];

2 — conformational defects in straightened sections of macromolecules formed by the kink-isomer, which in turn consists of a combination of the simplest isomers having trans- and gosh-conformations. It is customary to denote low-energy trans-conformations by the letter *t*, and higher-energy conformations by — *g*. Then the simplest kink conformer with alternation *ttt-g-t-g-ttt* is denoted by 2*g*1. According to the so-called crankshaft model [6], the kink-isomers appear as multidirectional steps on the macromolecule (Fig. 4, positions 2*a* and 2*b*). Conformers 2*g*1 are equilibrium defects. According to an

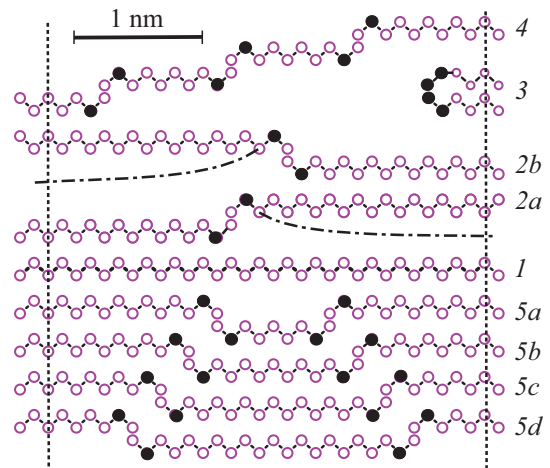


**Figure 4.** Elements of the structure of the intergranular part of the microfibril. Dotted lines — boundaries of crystal formations. The dark circles are marked with gauche isomers. Notations 1–5 — see text.

alternative model [12], the conformational defect in the straightened macromolecular segment is a step with a small portion of the chain adjusting as it moves away from the chain turning point (Fig. 4, positions 2*a* and 2*b*, dashed lines);

3 — irregular and regular loops formed by returning part of the molecules to the same crystallite from which they came. Irregular loops can be formed by a large number of gosh-conformers depending on the loop configuration; the smallest number in number of 4 gosh-conformers form regular loops or folds that form the crystal surface in lamellae (Fig. 4, position 3);

4 — bent pass-through molecules linking the crystallites together (Fig. 4, position 4). Their curvature is due to the presence of a single gosh-isomer on each side of neighboring crystallites. The curvature degree is determined by the number of gosh-isomers that can be located between these „surface“ gosh-isomers.

5 — the possibility of a structure formed by multidirectional steps or kink-isomers, referred to in the literature as „crankshaft“ [13] (Fig. 4, position 5*a*) is considered. A combination of these structures is assumed to exist (Figure 4, positions 5*b*–5*d*). This possibility is based on the fact that if the excess volume of one step is  $3/4\nu_0$ , where  $\nu_0$  — the volume of  $\text{CH}_2-$  group, then the excess volume of each of the nested steps is only  $1/4\nu_0$  [14], that is, in this case there is a cooperative effect.

It follows from the above list that the simplest gosh-isomer is an elementary defect that forms with „regular“ trans-isomers possible combinations of the polymer chain in a disordered area. However, this elementary defect, unlike the kink-isomer, is not an equilibrium defect and can only exist in combination with trans-isomers. Orientation stretching of the polymer at elevated temperatures is accompanied by an increase in the degree of crystallinity,

which is carried out by reducing the defectiveness of the disordered interlayer. The molecular mechanism of this process is related to the multidirectional diffusion of „kinks“ or double kinks along the polymer chain and their annihilation at the macromolecule ends or formation of a „crankshaft“ type defect and their combinations.

Clearly, each of the above combinations of isomers in the intergranular area makes a different contribution to the end-surface energy. Thus, for a kink defect (Fig. 4, positions 2a and 2b) containing two gosh-isomers, the surface energy will be determined by one gosh-isomer, since the step forms the elementary surface of two adjacent crystals. In the case of „crankshaft“ (Fig. 4, positions 5a–5d), the surface energy is already formed by two gosh-isomers; and finally, in the case of a regular fold (Fig. 4, position 3) — by four. The curved pass-through molecules that bind the crystallites together (Fig. 4, position 4) eventually straighten out due to kink diffusion during orientation stretching at elevated temperatures and turn into steps at the last stage. At this stage, the surface energy will also be determined by one gosh-isomer.

To determine the end-surface energy  $\sigma_e$  created by a single gosh-isomer, we must find the fraction of the formation energy of this defect  $\Delta E = 2.5$  kJ/mol per unit area  $\Delta S \approx 0.18$  nm<sup>2</sup> of the end surface of the chain. An estimate of the ratio  $\Delta E/\Delta S$  yields an end-surface energy value equal to  $\sigma_{e1} \approx 11$  erg/cm<sup>2</sup>. In the case of „crankshaft“ the surface energy generated by the two gosh-isomers already will be twice as much ( $\sigma_{e2} \approx 22$  erg/cm<sup>2</sup>).

The calculation of the distribution  $dH/dL$  by relations (1) and (4) for the fibrillar structure requires in addition to the known values of the end and lateral surface energies also the determination of the parameter  $l$ , i.e. the size of the microfibril in the cross section. It was noted above that, judging from the microphotograph in Fig. 1, b, the transverse dimensions of the microfibrils are 30–40 nm. Figure 3 (curves 2–5) shows the calculation of the distribution  $dH/dL$  for oriented PE samples with fibrillar PMC. The calculations used  $l = 40$  nm and  $\sigma_{e1} \approx 11$  erg/cm<sup>2</sup>.

Figure 3 shows a rather complex pattern of changes in the crystallite size distribution with orientation. In the first orientation step, a very sharp decrease in the size distribution range and a shift of this distribution towards lower size values compared to the original sample (curve 1) is observed in the formation area of the „neck“ (curve 2). This process is associated with the transition of the lamellar PMC characteristic of the original sample into a fibrillar one with small crystalline areas and a large fraction of the disordered part. Further orientation is accompanied by an increase in the size of the crystal areas, an increase in the blurring of the distributions and a decrease in the fraction of the disordered part (Fig. 3, curves 3–5).

To compare the obtained distributions with the X-ray data published in [11] and obtained, in turn, on the same samples, it is necessary to determine the weighted average

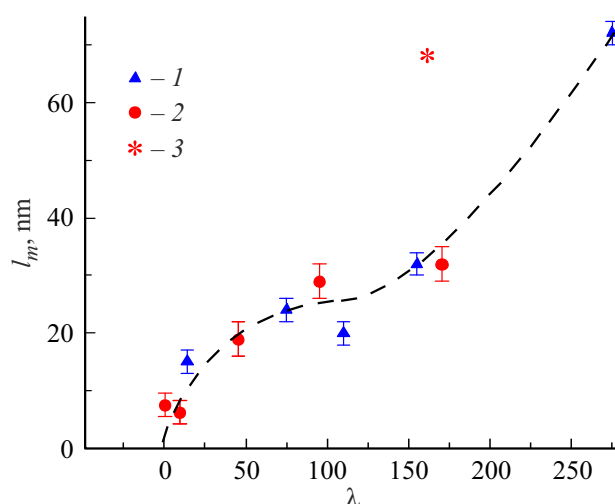


**Figure 5.** Dependences on the degree of orientation of the weighted average values of the longitudinal dimensions of crystallites from X-ray data (1) and calculated  $l_m$  at  $\sigma_{e1}$  (2) and  $\sigma_{e2}$  (3).

$l_m$  value in the distribution  $dH/dl_1$ . The value of  $l_m$  was determined by the ratio

$$l_m = \frac{\sum_i l_i (dH/dl_1)_i}{\sum_i (dH/dl_1)_i},$$

where  $l_i$  — the current value of  $l_1$  in the distribution;  $(dH/dl_1)_i$  — the current value of  $dH/dl_1$  at  $l_1 = l_i$ .

Fig. 5 shows the dependences of the weighted average values of the longitudinal crystallite sizes  $l_m$  on the degree of orientation of the original xerogel film obtained from the X-ray data (1) and the calculated values  $l_m$  (2, 3). It should be noted that there is some disagreement in the estimation of the longitudinal size of crystallites from the data of large-angle X-ray diffraction because of the different interpretation of the reasons for the broadening of reflex D002, by which the size of the crystallite is calculated. Some authors believe that the half-width of the D002 reflex depends solely on the crystallite size in the chain [15] direction, and in extremely oriented samples the longitudinal crystallite size can reach 60–80 nm. Others believe that when the elongation limits are reached in oriented films, a texture may arise in which crystallites are arranged along the fibril axis in a coherent manner, which leads to a sharp decrease in the half-width of the reflex. In such a case, the size of crystallites should not significantly exceed the size of crystallites formed at the stage of neck formation during rearrangement of folded crystallites into crystallites from straightened chains [16,17]. The figure shows that the X-ray (1) and the calculated distributions of longitudinal crystallite sizes (2) obtained from the calorimetric data practically fit into one dependence, which indicates that the first interpretation of the X-ray data is correct. In this calculation,  $\sigma_{e1}$  was used as the end-surface energy, i.e., the value of the end-surface energy created by one gosh-isomer. The figure shows that this dependence increases sharply at the initial stage, and then,

in the interval  $\lambda \approx 50\text{--}150$ , smoothly passes to saturation and becomes almost horizontal. Apparently, this process is related to the diffusion of kinks or double kinks that form the surface energy  $\sigma_{e1}$ , since they either annihilate when they reach the end of the chain or meet a double kink in the opposite direction and form a „crankshaft“-type structure. With a sufficiently large number of these elements in the limited space of the inter-crystalline area, their cooperation can occur in a structure similar to that shown in Fig. 4 (positions 5a–5d). In such a structure, the cooperative excess volume will be less than the sum of the excess volumes of the independent elements of this structure.

For ultra-high orientation elongation ( $\lambda \approx 270$ ) there is a sharp increase in  $l_m(\lambda)$  (Fig. 5). On the basis of relation (4), this rise can be due to two reasons. First, „by connecting“ in the process of orientation ordering of crystal formations with increased end-surface energy. A calculation using the value of the end-surface energy  $\sigma_{e2}$  formed by elements of the „crankshaft“-type structure does show (Fig. 5, position 3) a significant increase  $l_m$ . The participation in the ordering of crystal formations with even greater end-surface energy depends on the conditions of orientation drawing. Increasing the drawing temperature, which can already exceed the melting temperature of the equilibrium PE [18] crystal, leads to accelerated diffusion and annihilation of complex combinations of defects on the surface of crystal formations, which determine their high surface end-point energy.

The second reason for the sharp rise may be the dependence of the value of  $l_m$  on the transverse size of the crystallite, i.e. on the parameter  $l$  in the relation (4). Such a process should occur as the density of defects in the disordered interlayer decreases and the number of crystal bridges or straightened molecules in the trans-conformation between neighboring crystallites in the microfibril increases. In the limit case (at  $l_m \rightarrow \infty$ ) it follows from relation (4) that the parameter  $l$  tends to the value of 0.1–0.2 nm, i.e. the transverse size of the crystallite becomes comparable to the transverse size of a single polyethylene chain.

## 4. Conclusion

The method of calculating the size distribution of nanocrystalline elements of lamellar and fibrillar polymer permolecular structures proposed in this work allowed us to reveal a number of features of the process of orientation stretching of ultra-high molecular weight polyethylene. Based on the analysis of these features, a model describing the evolution of the disordered part of the polymer permolecular structure is proposed. The results of the calculation based on the weighted averages in the distribution obtained from the calorimetric data are consistent with the data obtained by the X-ray method.

## Conflict of interest

The authors declare that they have no conflict of interest.

## References

- [1] V. Marikhin, L. Myasnikova, Y. Boiko, E. Ivan'kova, E. Radovanova, P. Yakushev. Role of Reactor Powder Morphology in Producing High-strength High-modulus UHMWPE Fibres. In: Reactor Powder Morphology / Eds L. Myasnikova, P. Lemstra. Nova Publishers, Hauppauge, N.Y. (2011). Ch. 10. P. 235–294.
- [2] Yu.M. Boiko, V.A. Marikhin, O.A. Moskalyuk, L.P. Myasnikova. Physics of the Solid State **61**, 1, 182 (2019).
- [3] V.A. Marikhin, L.P. Myasnikova. Structural basis of high-strength high-modulus polymers. In: Oriented Polymer Materials / Ed. S. Fakirov. Huthig & Wepf Verlag-Zug, Heidelberg (1996). P. 38–98.
- [4] V.A. Marikhin, L.P. Myasnikova. Macromol. Chem. Macromol. Symp. B **41**, 209 (1991).
- [5] V.M. Egorov, A.K. Borisov, V.A. Marikhin, L.P. Myasnikova, E.M. Ivankova. Technical Physics **48**, 8, 43 (2022).
- [6] B. Wunderlich. Macromolecular Physics. Academic Press, London (1980). 363 p.
- [7] J.D. Hoffman. In: Treatise on Solid State Chemistry / Ed. N.B. Hannay. Plenum Press, N.Y. (1976). V. 3. P. 497–605.
- [8] K. Illers. Eur. Polym. J. **10**, 10, 911 (1974).
- [9] D.W. Van Krevelen. Properties of polymers correlations with chemical structure. Elsevier, N.Y. (1972). 480 p.
- [10] V.A. Marikhin, L.P. Myasnikova. The permolecular structure of polymers. Khimiya, L. (1977) (in Russian). 238 p.
- [11] V.A. Marikhin, L.P. Myasnikova, M.D. Uspensky. Polymer Science A **35**, 6, 686 (1993).
- [12] Yu.A. Gotlib, A.A. Darinsky, Yu.E. Svetlov. Physical kinetics of macromolecules. Khimiya, L. (1986). 272 p. (in Russian)
- [13] V.A. Marikhin. FTT **19**, 4, 1036 (1977) (in Russian).
- [14] P. Kaush. Polymer destruction. Mir, M. (1981). 440 p.
- [15] V.A. Marikhin, V.A. Berstein, V.M. Egorov, L.P. Myasnikova. Polymer Science A **28**, 9, 1983 (1986).
- [16] A.E. Azriel, V.A. Vasilyeva, L.G. Kazaryan. Polymer Science A **28**, 4, 809 (1986).
- [17] S.N. Chvalun, Yu.A. Zubov, N.F. Bakeev. Materials of the International Symp. on Chem. Fibers. Kalinin **1**, 26 (1990).
- [18] V.A. Berstein, V.M. Egorov, A.V. Savitsky, V.P. Demicheva. VMS **27**, 2, 113 (1985).